Chi-square test of the relativistic precession model through the neutron star IGR J17511-3057

Ivan Z. Stefanov
Deparment of Applied Physics, Faculty of Applied Mathematics and Informatics,
Technical university of Sofia,
8, Snt Kliment Ohridski Blvd, Sofia 1000, Bulgaria
izhivkov@tu-sofia.bg
(Submitted on 4 June 2023; Accepted on 25 August 2023)

Abstract. The aim of the current paper is to apply Bambi's method (Bambi, 2015) to a source which contains two or more simultaneous triads of variability components. The joint χ^2 variable that can be composed in this case, unlike some previous studies, allows the goodness of the fit to be tested. It appears that a good fit requires one of the observation groups to be disregarded. Even then, the model's prediction for the mass of the neutron star in the accreting millisecond pulsar IGR J17511-3057 is way too high to be accepted.
Key words: X-ray timing; quasi-periodic oscillations; pulsars; Millisecond accretion pulsar; IGR J17511-3057; accretion disk

1 Introduction

The presence of a simultaneous triad of quasi-periodic oscillations (QPOs) consisting of a pair of twin high frequency QPOs (HF QPOs), an upper and a lower one, and one low frequency QPO (LF QPO) in the spectra of low-mass X-ray binaries gives us the opportunity to measure with great precision the spin and mass of their central compact object (a black hole or a neutron star) as it was shown by Motta et al. (2014). They applied the relativistic precession model (RPM) to the simultaneous triad present in the X-ray power-density spectrum of the black hole binary GRO J1655-40. As a confirmation of the adequacy of the method and the model, the authors compare their estimation of the mass of the studied black hole to an earlier independent measurement and obtain very good agreement.

Soon after the work of Motta et al.(2014), Bambi (2015) studied the same stellar-mass black hole. He exploited the same simultaneous triad of QPOs and used the same model but proposed a different method, much more efficient from a numerical point of view, for calculation of the uncertainty of the estimated parameters – mass and spin. Bambi (2015) proposed a merit function that allows confidence level regions to be plotted in the joint mass-spin parameter space. It proves very useful for the estimation of the uncertainty of the parameters but it has zero degrees of freedom (dof) and cannot be treated as a standard χ^2 variable, so it does not allow us to apply a statistical test for the adequacy of the model.

The presence of simultaneous twin HF QPOs in the X-ray spectrum of BHBs is a rather rare event (Belloni et al. 2012; Ingram & Motta 2019). Simultaneous triads are even less frequent. GRO J1655-40 is, as far as we know, the only BH which has a confirmed simultaneous triad of narrow timing features. (This is why the QPOs of GRO J1655-40 are so vastly exploited.) Hence, it appears very unlikely to find a BHB with more than one simultaneous triad of QPOs in its X-ray power density spectrum.

One could increase the degrees of freedom of the merit function by including data from other, though incomplete, triads of QPOs. Such an incomplete

triad is present in the spectrum of GRO J1655-40 (Motta et al. 2014). It consists of an upper HF QPO and a C-type LF QPO. This pair has been added in the definition of a merit function, again with zero degrees of freedom, in Bambi & Nampalliwar (2016). It increases the number of terms by two but also requires the inclusion of one more parameter – the radius of the orbit at which it originates, which means that due to the inclusion of this pair the degrees of freedom rise by one. In this situation, the data allow one more free parameter to be added in the analysis, and hence deviations from the Kerr metric to be tested (Jing et al. 2016; Jiang et al. 2021). Another possibility to increase the number of studied free parameters is to supplement the simultaneous triad of QPOs with data from other measurements, such as the mass, as demonstrated by Bambi (2015) and Allahyari & Shao (2021). The authors of the latter paper use Bayesian approach and study the posterior probability distribution of the estimated parameters.

As it was recently shown in Ghasemi-Nodeli et al. (2020), the method of Bambi can be generalized to the case in which more than one triad of simultaneous QPOs is observed. In this paper, however, the datasets which contain several triads were not taken from observations but were rather synthesized.

Taking into account that the RPM can also explain the kHz QPOs, the analogue of the black hole HF QPOs, and the low-frequency variability components of neutron stars, we search for simultaneous triads among them. For recent observational interest in X-ray binaries see Nikolov (2020) and references therein. One possible candidate is the accreting millisecond X-ray pulsar IGR J17511-3057. It contains three triads of supposedly simultaneous variability components. Two of the frequencies in these triads could be classified as twin kHz QPOs, according to one of the interpretations given by Kalamkar et al. (2011). The third component in the groups of simultaneous observations of this source is not the C-type QPO that usually completes the triads described by the RPM, but rather a "hump" L_h variability component.

The aim of the current study is to apply the method presented in Bambi (2015) to obtain confidence level plots in the spin-mass parameter space for IGR J17511-3057. Our goal is to address several questions. First, do the estimates for the mass and the spin of this object from the different triads agree with each other?

The χ^2 variable, obtained from the combination of two triads of frequencies, contains six terms. In order to describe them, we need at least four parameters (in the case of Kerr metric) – the mass and the spin of the central object, and the radii of the two orbits on which the observed triads originate. Hence, the joint χ^2 variable has two degrees of freedom. If we combine all three of the simultaneous triads, the results is a χ^2 variable with four degrees of freedom. In these cases, we have the opportunity to apply the χ^2 goodness-of-fit test. So, the second question that we address is whether minimum value $\chi^2_{\rm min}$ allows us to accept the model?

There is one more condition that a feasible model must satisfy – giving a reasonable estimate for the mass of the neutron star, not exceeding the commonly accepted upper bound of three Solar masses.

We should clarify that in the current study black holes binaries and neutron stars binaries are treated equally in the sense that for the central object the same metric is used – Kerr, and the same model is applied for the description of the observed QPOs, namely the RPM. As it was shown in Stuchlík & Kološ

(2015), the former assumption is justified for the study of QPOs of black holes with a spin lower than 0.4.

The paper is organized as follows. The accreting millisecond pulsar IGR J17511-3057 and its narrow timing features are briefly presented in Section 2. A brief presentation of the RPM follows in Section 3. Section 4 is dedicated to the estimates of the spin relation coming from the different observations and to the role of uncertainties. Then come the Discussion and the Conclusion.

In this paper, all the masses are scaled with the Solar mass, the radii are scaled with the gravitational radius $r_{\rm g} \equiv GM/c^2$, the specific angular momentum $a \equiv J/cM^2$ and measure units in which $G = 1 = c$ are used.

2 IGR J17511-3057

The X-ray timing of the millisecond accreting pulsar IGR J17511-3057 has been studied by Kalamkar et al. (2011). They present the results from 71 pointed observations of this object with the RXTE PCA. To improve statistics close in time and color (We refer the reader to Ingram & Motta (2019) for more details on the color and the classification of the states of X-ray sources.), the observations have been combined into seven groups of 7 to 15. Following Belloni, Psaltis & van der Klis (2002), the authors fit the power spectrum of each group by a multi-Lorentzian function – a sum of several Lorentzians. Specifically, for the groups of observations 1, 2 and 7, the number of Lorentzians is five. Each Lorentzian corresponds to a different component in the power density spectrum (PDS). The different components have been identified with the help of correlation diagrams (Wijnands & van der Klis 1999; Psaltis et al. 1999; van Straaten et al. 2005) (See Section 3.3 in Kalamkar et al. (2011) for more details.).

In the current paper, we are searching for simultaneous triads of characteristic frequencies, namely a pair of twin kHz QPO (which are the analogue of the black hole HF QPOs for neutron stars) and one more low-frequency feature such as a low-frequency QPO or, as in this case, a "hump" feature L_h. Such components have been seen in three of the seven groups of observations – 1, 2 and 7. The presence of such triads would allow one to apply the relativistic precession model to describe them and, hence, to obtain estimates for the model parameters – the mass and the spin of the black hole and the radius of the orbit of origin of the observed features, resulting from the motion of inhomogeneities in the disk, as the model states. When it comes to the low-frequency sector, the relativistic precession model has been applied for the explanation of the C-type low-frequency QPOs, mostly, but also of the horizontal branch oscillations (HBOs) of Z sources (Stella & Vietri 1998; Stella, Vietri & Morsink 1999; Stella & Possenti 2009) and L_h of the atoll source 4U 1608–52 (van Straaten et al. 2003).

The studied source IGR J17511-3057 has no LF QPOs in groups 1, 2 and 7. We chose them in particular due to the presence of twin kHz QPOs. The only possibility that remains in this case, is to complement the desired triads with the hump features L_h that are present in these groups.

The values of the characteristic frequencies and their uncertainties are provided in Table 1. As Kalamkar et al. (2011) state, the interpretation of the

Table 1. Features in the PDS of IGR J17511-3057

group	$\nu_{\max}$, (Hz)	Identification
1	251.8 ± 13.9	L_u
	139.7 ± 4.2	L_l
	6.4 ± 0.6	L_h
2	272.2 ± 13.9	L_u
	129.9 ± 11.0	L_l
	5.2 ± 0.2	L_h
7	179.9 ± 14.9	L_u
	72.5 ± 4.9	L_u
	13.7 ± 2.5	L_h

highest frequency QPOs is uncertain. One possibility is that these pairs represent twin kHz QPOs. It is possible, however, that the second highest frequency QPOs are hecto Hz QPOs. There is also one more scenario. According to Scenario 4 in Kalamkar et al. (2011), the two highest frequency QPOs in groups 1 and 2 are hecto Hz QPOs, while the two highest frequencies of group 7 cannot be identified.

We also have to admit that, according to Kalamkar et al. (2011), the identification of the L_h features is also uncertain.

3 Relativistic precession model

Stella and Vietri proposed the RPM (Stella & Vietri 1998; Stella, Vietri & Morsink 1999; Stella & Possenti 2009) in their attempt to explain the correlation between the LF QPOs and the lower kHz QPOs that has been reported by Psaltis, Belloni & van der Klis (1999) and van der Klis (2006) for a large number of neutron-star sources. Soon after that they adapted it to black holes (Merloni et al. 1999).

According to the RPM, which belongs to the group of the hot spot models, the X-ray flux of black holes and neutron stars is modulated by the motion inhomogeneities in the inner region of the accretion disk, where most of the energy is released. The frequencies that appear in the power density spectra are related to the geodesic orbital, epicyclic and precession frequencies.

We could say that the RPM is a collection of three models – one for the low-frequency narrow timing components such as a LF QPO, a horizontal branch oscillation or a hump component $\nu_{\rm h}$, and two more – the lower $\nu_{\rm l}$ and the upper $\nu_{\rm u}$ twin kHz QPOs. These frequencies are attributed to the nodal precession $\nu_{\rm nod} = |\nu_\phi - \nu_\theta|$, the periastron precession $\nu_{\rm per} = \nu_\phi - \nu_{\rm r}$ and the orbital ν_ϕ frequencies, respectively.

The radial and vertical epicyclic frequencies, $\nu_{\rm r}$ and ν_θ, have been obtained for the Kerr space-time in Aliev & Gal'tsov (1981), Aliev, Gal'tsov & Petukhov (1986) and Aliev, Esmer & Talazan (2013). They are provided in the Appendix.

4 Modeling of data

4.1 Each triad separately

In this section, we follow the idea presented in Bambi (2015) and define the following merit function for the i-th triad of QPOs, where the index i designate

the groups of observations which contain simultaneous triads, namely 1st, 2nd and 7th,

$$\chi^2_{\rm i}(a, M, r_{\rm i}) = \frac{\left(\nu_{\rm h} - \nu^{\rm obs}_{\rm h,i}\right)^2}{\sigma^2_{\rm h}} + \\ + \frac{\left(\nu_{\rm l} - \nu^{\rm obs}_{\rm l,i}\right)^2}{\sigma^2_{\rm l}} + \frac{\left(\nu_{\rm u} - \nu^{\rm obs}_{\rm u,i}\right)^2}{\sigma^2_{\rm u}}. \tag{1}$$

Here, the observed frequency of the hump feature is designated as $\nu^{\rm obs}_{\rm h,i}$, while those of the two kHz QPOs are, respectively, $\nu^{\rm obs}_{\rm l,i}$ and $\nu^{\rm obs}_{\rm u,i}$. The model frequencies are $\nu_{\rm h}$, $\nu_{\rm l}$ and $\nu_{\rm u}$, respectively.

The merit function (1) contains three terms – one for each of the frequencies in the triad. The optimal values of the parameters M, a, and the radius $r_{\rm i}$ of the orbit on which the i-th pair originates are those which minimize (1). The number of optimized parameters is equal to the number of terms, so the merit function has zero degrees of freedom in this case. It is not an authentic χ^2 variable.

As demonstrated in Bambi (2015), we can define a χ^2 variable (with two rather than three degrees of freedom) which can be used to obtain confidence level regions in the plane of the parameters a and M in the following way:

$$\Delta\chi^2_{\rm i} \equiv \chi^2_{\rm i} - \chi^2_{\rm i,min}. \tag{2}$$

Here $\chi^2_{\rm i,min}$ is the minimum value of (1), which is actually zero whenever the system defined by the three frequencies and the three observed values has a solution, while $\chi^2_{\rm i}$ is the value of (1) obtained for given values of M and a and minimized with respect to $r_{\rm i}$. (The geometrical interpretation of this condition is briefly commented in Stefanov (2020a).) The χ^2 variable (2) has three terms and depends on three parameters. Once again, two of the parameters, M and a, can vary freely, but the value of $r_{\rm i}$ is chosen so as to minimize $\Delta\chi^2_{\rm i}$. The minimization of $\Delta\chi^2_{\rm i}$ with respect to one of the parameters reduces the degrees of freedom by one, or dof $= 3 - 1 = 2$. For more details on the χ^2 goodness-of-fit test we refer the reader to Scott P.[1], Press et al. (2007), Bevington & Robinson (2003) and Stefanov & Tasheva (2022).

In 68.3% of the cases the χ^2 variable $\Delta\chi^2_{\rm i}$ takes values lower than or equal to 2.3. This confidence level, corresponding to 1-σ, defines a region in the space of parameters M and a. Its boundary is represented by an ellipse in Fig. 1 for each one of the three groups of observations – 1, 2 and 7. Here and bellow we choose to present only the 1-σ confidence regions and omit the 2-σ and 3-σ ones, as customary, in order to avoid cumbersome figures. Besides, in this work, we are searching for conflicts between the predictions coming from

[1] Prof. Peter Scott has a document entitled "*Physics 133 Lab manual*" on his personal webpage `http://scott.physics.ucsc.edu/` which is an excellent pedagogical text on the chi-square goodness-of-fit test.

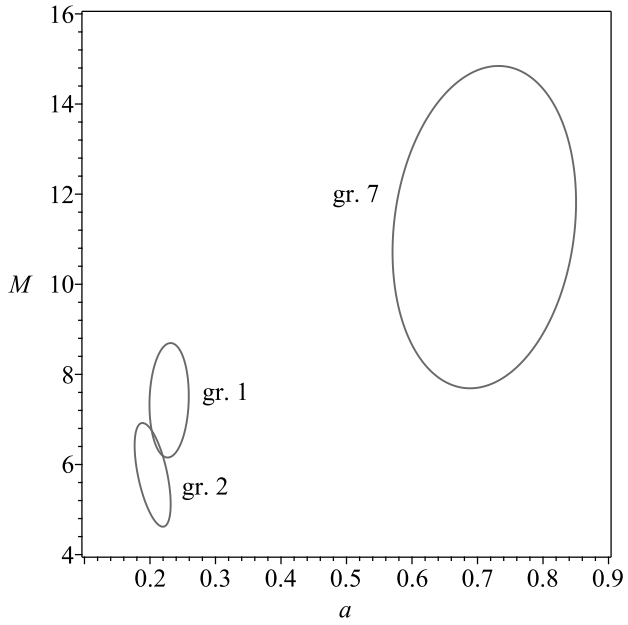

Fig. 1. The 1-σ covariance plots obtained with the data from the triads from groups 1, 2 and 7.

the different measurements which are more likely to manifest themselves when more conservative constraints on the parameters are used. For the production of the confidence regions (the error ellipses), we follow the procedure from the prominent book "Numerical Recipies" (Press et al. 2007) and explained by prof. Peter Scott (Scott P.) in which the χ^2 variable is expanded to the leading, actually second, order terms. As a result the confidence regions are ellipses. This method has been also followed by Maselli et al. (2017), for example. Bambi (2015) and most of the works that cite him choose a different approach and plot the "full" 2D confidence level regions which have irregular shape. This approach can also be seen in Kjurkchieva et al. (2020) where constraints for the possible mass ratios and inclinations of two short-period eclipsing stars are given.

As it can be seen in Fig. 1, the confidence level regions derived from the different groups of observations, which can be treated as three independent experiments or measurements, do not overlap. Groups 1 and 2 are in partial agreement but group 7 appears as an outlier.

The constraints on a resulting from groups 1 and 2 are moderate and comply with the requirement $a \leq 0.4$, which guarantees the validity of the Kerr metric for the evaluation of the epicyclic frequencies of a neutron star. Group 7, however, predicts much higher values for the spin, which give us reason to question the applicability of Kerr metric in this case. For all of the

three measurements, the constraints on M are notably high for a neutron star. Even the stiffest equations of state predict masses lower than 3 Solar masses.

4.2 Combinations of three triads

In this subsection, we take advantage of the fact that the X-ray spectrum of IGR J17511-3057 contains several triads of QPOs which can be combined. Unlike the previous case, the joint merit function that results from the combination of the three pairs of independent observations this time, is an authentic χ^2 variable with four degrees of freedom, a fact which gives us the opportunity to test the validity of the model. The combination of all three triads of QPOs allows us to define the following χ^2 variable

$$\chi^2_{\rm three}(a, M, r_1, r_2, r_7) = \sum_{\rm i=1,2,7} \chi^2_{\rm i}, \tag{3}$$

where the $\chi^2_{\rm i}$-s are given by equation (1). It is a χ^2 variable with dof $= 4$, since it has nine terms and five parameter – a, M and the radii of origin of the three triads in the combination r_1, r_2 and r_7 which are optimized. The minimum value of $\chi^2_{\rm three}$ (3) is

$$\chi^2_{\rm three,min} = 22.9. \tag{4}$$

The quality of the fit appears to be poor. The critical value for a χ^2 variable with dof $= 4$, at 5% level of confidence, is 9.5, while the minimum value (4) that we obtain 22.9 is significantly higher than it.

Confidence limits of the estimated values of a and M can be obtained, just as in the previous subsection, with the help of the χ^2 variable

$$\Delta\chi^2_{\rm three} \equiv \chi^2_{\rm three} - \chi^2_{\rm three,min}. \tag{5}$$

The error ellipse in the $a - M$ parameter space obtained with (5) is given in Fig. 2 with the thick solid line.

As it can be seen in Fig. 2, the mass estimation, given by the projection of the error ellipse on the vertical axis, is again too high for a neutron star. The spin is moderate, lower than 0.4, and justifies the application of the Kerr metric.

Interestingly, the thick solid error ellipse is pulled to the left, towards the moderate values of the spin, even though group 7 is also taken into account. This can be attributed to the significantly smaller uncertainties and, hence, greater weights of the hump components in groups 1 and 2, which favor moderate spin, in comparison to that of group 7, which requires high spin.

4.3 Combinations of two triads

The reason for the poor fit from the previous subsection might be the presence of an oultlier, such as group 7, for example. In order to test this possibility we

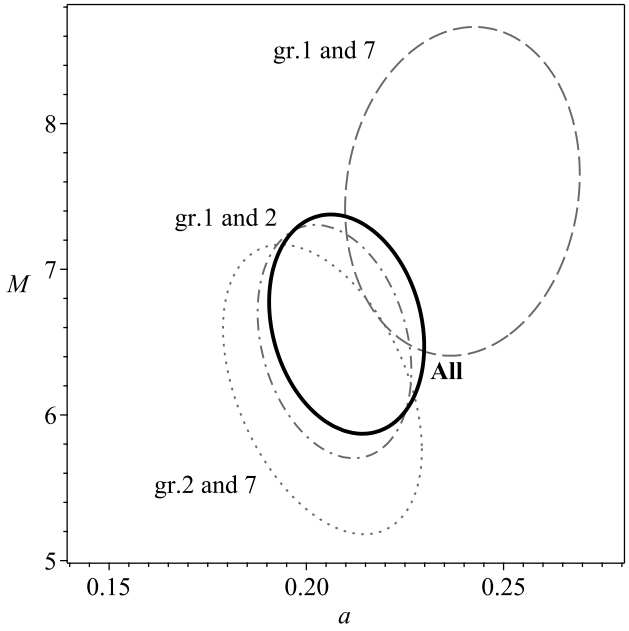

Fig. 2. The 1-σ covariance plot obtained by the combination of two and three triads of QPOs.

remove one of the groups and define another merit function by the combination of two different groups of observations

$$\chi^2_{\rm two}(a, M, r_{\rm i}, r_{\rm j}) = \chi^2_{\rm i} + \chi^2_{\rm j}, \tag{6}$$

where, the $\chi^2_{\rm i}$-s are given by equation (1), ${\rm i, j} = 1, 2, 7$ and ${\rm i} \neq {\rm j}$. We take into account all possible combinations of two groups of observations, namely 1 and 2, 1 and 7 and 2 and 7, and obtain three χ^2 variables, denoted as $\chi^2_{\rm two}$. Each of them has six terms and is optimized with respect to four parameters – a, M and the radii of origin of the two triads in the combination, i.e. dof $= 6-4 = 2$.

The minimum values of the χ^2 variable obtained by the combination of groups 1 and 2, 1 and 7 and 2 and 7, respectively are:

$$\chi^2_{\rm two,12,min} = 3.91, \tag{7}$$

$$\chi^2_{\rm two,17,min} = 17.1, \tag{8}$$

$$\chi^2_{\rm two,27,min} = 20.2. \tag{9}$$

For two degrees of freedom, the critical value of the χ^2 variable corresponding to a 5% confidence level is 5.991. As it can be seen form eqs. (7)–(9) the inclusion of groups 7 in the combination results in values for $\chi^2_{\rm min}$ which are

higher than the critical one. In other words, groups 1 and 2 can be reconciled (see the value of (7)), but, as apparent from (8) and (9), (7) is not in agreement with them.

Just as in the previous cases, for all combinations, we obtain 1-σ confidence ellipses in the $a - M$ space through level plots of the following function

$$\Delta\chi^2_{\rm two} \equiv \chi^2_{\rm two} - \chi^2_{\rm two,min}, \tag{10}$$

expanded in Taylor series up to second order terms in a and M. The error ellipses are again given in Fig. 2, where the ellipse obtained with groups 1 and 2 is represented by a dash-dotted line, with 1 and 7 by a dashed line and with the last combination – 2 and 7, by a dotted line.

The confidence regions obtained with groups 1 and 7 (dotted line) and groups 2 and 7 (dashed line) barely overlap. The dash-dotted line which represents confidence region resulting from the combination of groups 1 and 2 overlaps partially with both previous. All of the thin-line ellipses overlap partially with the solid one which is a result of the combination of all three of the considered groups of observations.

5 Discussion

The aim of the current paper is to apply Bambi's method (Bambi 2015) to a source which contains two or more simultaneous triads of variability components. The joint χ^2 variable that can be composed in this situation is an authentic one, in a sense that it has non-zero degrees of freedom, a fact which allows the goodness of the fit to be tested. For this purpose, we chose the accreting millisecond X-ray pulsar IGR J17511-3057, whose X-ray spectrum contains three supposedly simultaneous triads of variability components described in Section 2.

The following aspects of the model are tested: the metric and the association of the observed frequencies with orbital frequency, periastron precession frequency and the nodal precession frequency, as stated by the relativistic precession model. First, the space-time in the vicinity of the central object can be described by Kerr metric. This of course is questionable for neutron stars. However, as Stuchlík & Kološ (2015) show, the Kerr metric is applicable for the calculation of the epicyclic frequencies of neutron stars with moderate spin, $a < 0.4$. This constraint is satisfied by the individual predictions for the spin of the studied object obtained with groups 1 and 2 but not with group 7. All constraints obtained by the joint χ^2 of two or three groups satisfy the cited theoretical constraint on the spin in question.

Second, it is common to describe, according to the RPM, the HF QPOs of black holes and the kHz QPOs of neutrons stars by the orbital frequency and periastron precession frequency. However, it is less common to apply the nodal precession frequency to the hump component, instead of the usual C-type LF QPOs . An example for the latter can be seen in van Straaten et al. (2003).

The limitations on the experimental side of this study are mainly related with the choice of the source. Indeed, the presence of three triads of simultaneous variability components in the X-ray PDS of IGR J17511-3057 which can be modeled by the relativistic precession model makes it an excellent

choice. However, as the Kalamkar et al. (2011) state and as we reiterate here in Section 2, the identification of the features in the X-ray PDS is uncertain. Other sources that could serve to test the feasibility of the RPM through the methodology proposed in this study are: 4U 1728-34, XTE J1807-294 and 4U 1608-52, to name a few.

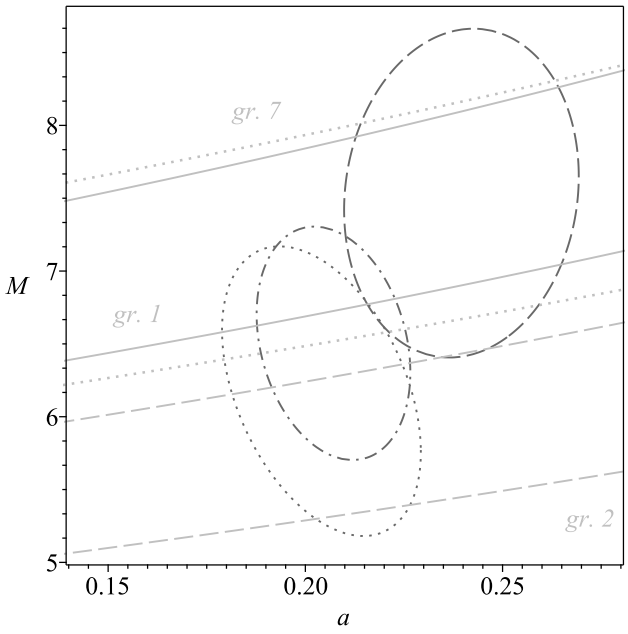

Fig. 3. The predictions for the $a - M$ relation coming from groups 1 and 2 from (Stefanov, 2016.

The results obtained from the current study are as follows. The individual predictions of groups 1 and 2 for the mass and spin of the object are in marginal agreement – the confidence regions obtained with them barely overlap at the chosen level of confidence of 68.3%. The prediction of group 7 is in conflict with them. The individual and joint predictions for the spin coming from groups 1 and 2 are moderate, providing no reason to question the applicability of Kerr metric. Group 7 alone predicts spin that is significantly high to justify the use of Kerr metric.

The joint χ^2 of groups 1 and 2 takes acceptable minimum value $\chi^2_{\rm min}$, i.e. these two observations can be reconciled. The inclusion of group 7 in the combinations of two or three groups deteriorates the goodness of the fit. In these cases, the minimum values of the joint χ^2 are much grater than the critical value for the chosen confidence level of 5% and favors the rejection of the model. It appears that group 7 is an outlier.

With all version of the merit function that we use here, the estimates of the mass are much higher than the upper theoretical bound for a neutron star.

Similar overestimation of the mass has been reported also for the accreting millisecond pulsar XTE J1807-294 (Tasheva & Stefanov 2019, 2021). This drawback of the RPM occurs also with Z sources but not with atoll sources. See Lin et al. (2011) and Stefanov (2020a).

How do the results from this study compare with earlier ones (Stefanov 2015, 2016; Tasheva 2018)? The two latter studies provide constraints only for the mass, not for the spin because $\nu_{\rm h}$ was not taken into account. The degeneracy of the spin-mass relation that occurs when only two of the frequencies in the triad are use is also reported by Török et al. (2010, 2011, 2012) and Stefanov (2016) and studied in more details in Stefanov (2020b). In the two studies different methodology for the estimation of the uncertainty of the mass was used which results in small differences in the predictions for the masses. Stefanov (2016) states – for a given value of the spin the predictions of groups 1 and 2 for the mass do not agree with each other. This result is reproduced here in Fig. 3. The stripes which represent the predictions coming from group 1, with solid gray boundaries and from group 2 – dashed gray boundaries, do not overlap. They could be reconciled, however, if the uncertainty in the predictions for the spin was taken into account.

In Stefanov (2016) agreement between groups 1 and 7 was ascertained. The latter agreement is questionable since it appears only for very high spins, a situation for which Kerr metric is not justified (Stuchlík & Kološ 2015). This agreement disappears when the third frequency is included and the degeneracy is broken as a result.

In Fig. 3 the ellipses coming from the combinations of two groups of observations from the present study are also given. It can be clearly seen that the joint prediction of groups 1 and 2, given by the dash-dotted ellipse overlaps with both the group 1 and group 2 stripes.

In Stefanov (2015) and Tasheva (2018) the $\nu_{\rm u} - \nu_{\rm l}$ correlation is modeled and χ^2 minimization is used to obtain constraints on the mass and spin of the neutron star IGR J17511-3057. In these papers, only the pairs of the kHz QPOs present in power-density spectrum, i.e. the low-frequency features are omitted. The aim of Tasheva (2018) is to compare several alternative models for the kHz QPOs. As the author states, all of the studied models fail to fit the ensemble behavior of the lower and upper frequency QPOs, according to the χ^2 test. All but one of the considered models predict too high masses.

A solution of the problem with the overestimation may come from alternative gravity theories in which, for example, a fundamental scalar field is present. We refer the reader to Staykov et al. (2019, 2023), Marinov (2020), Kuan et al. (2021) and references therein for recent results on neutron stars coupled to a fundamental scalar fields. Some cosmological implications of massless and massive fundamental scalar fields can be found in Arik & Susam (2021) and Aditya & Divya Prasanthi (2023), respectively.

Another idea for future study is to define a joint χ^2 variable which contains frequencies from different incomplete simultaneous triads. A method which could be applicable to situations of insufficient data.

6 Conclusion

If we assume that one or all of the frequencies in group 7 are outliers and remove this group from our considerations then minimum value of the joint χ^2 variable that we obtain is acceptable and does not doubts the feasibility of the model.

The constraints for the spin of the central neutron star in IGR J17511-3057 obtained with groups 1 and 2, both the individual and joint, are moderate and justify the use of the Kerr metric.

The major deficiency of the model is, as it appears, the prediction for the mass of the neutron star. The constraints that we obtain in all of the cases, including those with the more favorable groups of observations 1 and 2, are much higher than the upper bound for a neutron star of three Solar masses.

Acknowledgments

I.S. would like to thank his wife for the support, Dr. Sava Donkov and Dr. Radostina Tasheva for the numerous discussions on the subject and prof. Stoytcho Yazadjiev for drawing his attention to the subject of QPOs.

References

Aditya, Y., & Divya Prasanthi, U. Y., 2023, BlgAJ, 38, 52
Aliev, A. N., & Gal'tsov, D. V., 1981, GReGr, 13, 899
Aliev, A. N., & Gal'tsov, D. V., & Petukhov, V. I., 1986, Ap&SS, 124, 137
Aliev, A. N., Esmer, G. D., & Talazan, P., 2013, CQGra, 30, 045010, arXiv:1205.2838 [gr-qc]
Allahyari, A., & Shao, L., 2021, JCAP, 10, 003
Arik, M., & Amon Susam, L., 2021, Rom. Rep. Phys., 73, 108
Bambi, C., 2015, Eur. Phys. J. C, 75, 162
Bambi, C., & Nampalliwar, S., 2016, Europhys. Lett., 116, 30006
Belloni, T., Psaltis, D., & van der Klis, M., 2002, ApJ, 572, 392
Belloni, T. M., Sanna, A., & Méndez, M., 2012, MNRAS, 426, 1701
Bevington, P., & Robinson, D. K., 2003, "*Data Reduction and Error Analysis for the Physical Sciences*", 3rd edn. (McGraw-Hill)
Chen, S., Wang, M., & Jing, J., 2016, Classic. Quant. Grav., 33, 195002
Ghasemi-Nodehi, M., Lu, Y., Chen, J., & Yang, C., 2021, EPJ C, 80, 504
Ingram, A. R., & Motta, S. E., 2019, New Astronomy Reviews, 85, 101524
Jiang, X., Wang, P., Yang, H., & Wu, H., 2021, EPJ C, 81, 1043
Kalamkar, M., Altamirano, D., & van der Klis, M., 2011, ApJ, 729, 7
Kjurkchieva, D., Popov, V., Eneva, Y., & Petrov, N., 2020, BlgAJ, 32, 71
Kuan, H.-J., Singh, J., Doneva, D. D. , Yazadjiev, S. S., & Kokkotas, K. D., 2021, Phys. Rev. D, 104, 124013
Lin, Y.-F., Boutelier, M., Barret, D., & Zhang, S.-N., 2011, ApJ, 726, 74
Marinov, K., 2020, BlgAJ, 33, 114
Maselli, A., Pani, P., Cotesta, R., Gualtieri, L., Ferrari, V., & Stella L., 2017, ApJ, 843, 25
Merloni, A., Vietri, M., Stella, L., & Bini, D., 1999, MNRAS, 304, 155
Motta, S. E., Belloni, T. M., Stella, L., Munoz-Darias, T., & Fender, R. 2014, MNRAS, 437, 2554
Nikolov, Y., 2020, BlgAJ, 32, 125
Press, W. H., Teukolsky, S. A., Vetterling, W. T., & Flannery, B. P., 2007, "*Numerical Recipes: The Art of Scientific Computing*", 3rd edn. (Cambridge University Press)
Psaltis, D., Belloni, T., & van der Klis, M., 1999, ApJ, 520, 262
Staykov, K. V., Doneva, D. D., & Yazadjiev, S. S., 2019, ApSS, 364, 178
Staykov, K. V., Doneva, D. D., Heisenberg, L., Stergioulas, N., & Yazadjiev, S. S., 2023, Physical Review D, 108, 024058

Stefanov, I. Z., 2015, in Proceedings of the scientific conference "Dni na fizikata – TU-Sofia", 21-25 April 2015 ("Days of physics – Technical university of Sofia"), p. 89, (in Bulgarian), ISSN 1313-9576, https://is.gd/hlqg7j
Stefanov, I. Zh., 2016, AN, 337, 246
Stefanov, I. Z., 2020a, in Proceedings of the scientific conference "Dni na fizikata – TU-Sofia", 01-04 April 2020 ("Days of physics – Technical university of Sofia"), p.74, arXiv:2007.13606
Stefanov, I. Z., 2020b, IJMPD, 29, 2050110
Stefanov, I. Z., & Tasheva, R. P., 2022, Rom. Rep. Phys., 74, 105
Stella, L., & Possenti, A., 2009, SSRv, 148, 105
Stella, L., & Vietri, M., 1998, ApJ, 492, L59
Stella, L., Vietri, M., & Morsink, S., 1999, ApJ, 524, L63
Stuchlík, Z., & Kološ, M., 2015, GReGr, 47, 23
Tasheva, R., 2018, BlgAJ, 28, 95
Tasheva, R., & Stefanov, I., 2019, AIP Conference Proceedings, 2075 , 090007
Tasheva, R., & Stefanov, I., 2021, BlgAJ, 34, 103
Török, G., Bakala, P., Srámková, E., Stuchlík, Z., & Urbanec, M., 2010, ApJ, 714, 748
Török, G., Kotrlova, A., Sramkova, E., & Stuchlík, Z., 2011, A&A, 531, A59
Török, G., Bakala, P., Sramkova, E., Stuchlík, Z., Urbanec, M., & Katerina, G., 2012, ApJ, 760, 13
van der Klis, M., 2006, AdSpR, 38, 2675
van Straaten, S., van der Klis, M., & Méndez, M., 2003, ApJ, 596, 1155
van Straaten, S., van der Klis, M., & Wijnands, R., 2005, ApJ, 619, 455
Wijnands, R., & van der Klis, M., 1999, ApJ, 514, 939

Appendix

Explicit formulas for the orbital frequency ν_ϕ and the two epicyclic frequencies – the radial ν_r and the vertical ν_θ (Aliev & Gal'tsov 1981; Aliev, Gal'tsov & Petukhov 1986; Aliev, Esmer & Talazan 2013)

$$\nu_\phi = \left(\frac{1}{2\pi}\right) \frac{M^{1/2}}{r^{3/2} + aM^{1/2}} \ , \tag{11}$$

$$\nu_r^2 = \nu_\phi^2 \left(1 - \frac{6M}{r} - \frac{3a^2}{r^2} + 8a\frac{M^{1/2}}{r^{3/2}}\right), \tag{12}$$

$$\nu_\theta^2 = \nu_\phi^2 \left(1 + \frac{3a^2}{r^2} - 4a\frac{M^{1/2}}{r^{3/2}}\right), \tag{13}$$

valid for the Kerr black hole. A change in the orientation of the orbit (direction of rotation of the hot spot) is equivalent to a change of the direction of rotation of the central object, i.e. a change in the sign of a.